

# Regularized Integral Equations and Curvilinear Boundary Elements for Electromagnetic Wave Scattering in Three Dimensions

Joseph C. Chao, *Student Member, IEEE*, Yijun J. Liu, Frank J. Rizzo,  
Paul A. Martin, and Lalita Udpa, *Senior Member, IEEE*

**Abstract**—The boundary integral equations (BIE's), in their original forms, which govern the electromagnetic (EM) wave scattering in three-dimensional space contain at least a hypersingularity ( $1/R^3$ ) or a Cauchy-singularity ( $1/R^2$ ), usually both. Thus, obtaining reliable numerical solutions using such equations requires considerable care, especially when developing systematic numerical integration procedures for realistic problems. In this paper, regularized BIE's for the numerical computation of time-harmonic EM scattering fields due to arbitrarily-shaped scatterers are introduced. Two regularization approaches utilizing an isolation method plus a mapping [1] are presented to remove all singularities prior to numerical integration. Both approaches differ from all existing approaches to EM scattering problems. Both work for integral equations initially containing either hypersingularities or Cauchy-singularities, without the need to introduce surface divergences or other derivatives of the EM fields on the boundary. Also, neither approach is limited to flat surfaces nor flat-element models of curved surfaces. The Müller linear combination [2] of the electric- and magnetic-field integral equations (EFIE) and (MFIE) is used in this paper to avoid the resonance difficulty that is usually associated with integral equation-based formulations. Some preliminary numerical results for EM scattering due to single and multiple dielectric spheres are presented and compared with analytical solutions.

## I. INTRODUCTION

THERE is a rich literature on boundary integral equation (BIE) methods for the numerical solution of electromagnetic (EM) scattering by three-dimensional, homogeneous scatterers [3]–[8]. For instance, [9] has successfully created a thin-coating formulation for solving scattering problems by perfectly conducting bodies with thin dielectric coating. Also, [10] has solved the scattering problem due to lossy dielectric bodies using planar, triangular elements. Some fundamental papers which discuss various BIE formulations to avoid resonance problems include [2], [8], and [11]. Most of these papers are based on either the combined field integral equations (CFIE's, commonly referred as PMCHW formulation [11]) or the Müller linear combination equations (MLCE's) [12]. For simpler two-dimensional problems, the authors of [13] have solved the biological scattering problems using BIE's.

Despite the rich literature, anyone with a difficult three-dimensional problem of EM scattering would find few papers for guidance which do not require a hypersingular kernel to be transformed to a lower singularity in trade for a surface divergence or other derivatives of the EM fields on the surface. In general, the BIE's for EM scattering contain three-kernel functions associated with each integral equation. If the unknown density functions are expressed in terms of the tangential fields, then the three-kernel functions contain a hypersingularity, a strong (Cauchy) singularity, and a weak singularity. In the MLCE's, however, there are two weakly singular-kernel functions and one Cauchy singular-kernel function. This comes about from the analytical cancellation of the hypersingular kernels and is only true for MLCE's.

In most of the literature we surveyed, the strongly singular integrals have been evaluated in the sense of Cauchy principal value (CPV). The only exception is [3] where a technique similar to our regularization procedure was applied to reduce the order of the strongly singular kernel functions. This technique, however, can be considered as a special case of our regularization procedure. The major disadvantage with CPV's is that they are difficult to compute numerically, especially for curved surfaces. As a result, CPV's are usually computed analytically assuming that the surface where they are defined is locally flat, or even more restrictive; piecewise flat elements are used to model the entire curved surface. Indeed, in all but one paper of the literature we surveyed, only flat planar elements are used everywhere.

In most cases, the hypersingular integral is avoided in one of two ways: The first is to transfer one of the derivatives from the hypersingular kernel function onto the density function. This results in a strongly singular integral with the unknown being the surface divergence of the density function. The appearance now of the surface divergence of the density (or any of its derivatives), rather than the density itself, is less desirable analytically and strategically, especially for systematic numerical computing. Also, with this procedure, there remains a strong (Cauchy) singularity which, admittedly, presents a manageable computational problem, provided one adheres to computer modeling with flat boundary elements. We submit, however, having to model a given difficult problem with sharply curved geometry using flat elements is a severe limitation. The second way is to analytically transform this surface divergence term

Manuscript received August 8, 1994; revised May 8, 1995.

The authors are with the Center for Nondestructive Evaluation, Iowa State University, Ames, IA 50011 USA.

IEEE Log Number 9415641.

into the normal component of the fields. This results in more unknowns to be solved and also a strongly singular kernel function. In a recent paper [14] to solve a simpler two-dimensional problem, a one-term subtraction was done to reduce the hypersingular kernel to a Cauchy singular kernel. Conventional methods are then applied to compute the Cauchy singular integral. Using this approach, it was seen that the approximation for the off-diagonal matrix elements close to the self-patch is not very good.

How to remove the above inconvenience, restrictions, and computational burdens via regularization procedures, which are valid for curved elements, is the thrust of this paper. The present regularization process first analytically reduces the order of the singularity of the kernel function from either strongly singular or hypersingular to weakly singular. Next a mapping from Cartesian to local coordinates is performed. The mapping process analytically transforms the weakly singular integrals into regular integrals which are then numerically computed using ordinary Gaussian quadrature. In this paper, the BIE's we begin with came from the MLCE formulation. This formulation provides a set of uniquely solvable BIE's at all frequencies [2]. Another benefit of the MLCE's is that the hypersingularities in the original BIE's are canceled in the combination, such that only a simpler version of our regularization procedure is required. With the most general form of our regularization procedure other formulations such as the CFIE's, may also be used.

The formulation in the next section refers explicitly to more than one scatterer, and the numerical examples involve scattering from two dielectric spheres. Numerical results for the single scattering case are also included to show the accuracy of the model as the permittivity and the radius of the scatterer increases. Conceptually, solving multiple-scattering problems using BIE's is a straightforward extension of solving single-scattering problems where the collocation and integration are over the union of the individual surfaces. As a practical matter, however, as the scatterers get closer to one another, the high-order kernel function will start to dominate and the solution will quickly diverge if the kernel functions are left in their original form. This type of singularity will be referred as near-singularity. The near-singularity typically creates a numerical problem for BIE formulations based on CPV interpretations where the singularity is considered for points on the same surface, but not for points on separate surfaces. Thus, typically, multiple-scattering problems due to arbitrarily-shaped objects are solved for cases where the scatterers are far apart. Furthermore, other approximate methods exist where only a limited number of wave interactions are considered [15], [16] or by assuming that the total scattered field is the sum of the individual scattered field with no interaction between the individual scatterers [17], [18]. Rarely are there cases where the full interaction effects are accounted for in the multiple scattering problem with arbitrarily-shaped scatterers close to one another. The present regularization gives rise to well-behaved kernels in the BIE's for closely-spaced scatterers.

Note that other numerical techniques such as the finite element method (FEM) and the finite difference method (FDM)

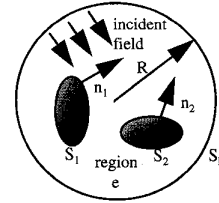


Fig. 1. Two-scatterer problem.

face difficulty when dealing with multiple scattering problems. Since FEM and FDM are both field-approximate methods, the domain to be discretized includes the volume of each scatterer plus the region exterior to the scatterers. This is a computationally expensive way of solving three-dimensional scattering problems. The BIE method is an ideal alternative since the BIE requires the discretization of only the bounding surface of the scatterers. This is much easier to do than discretizing the exterior domain, especially between the scatterers which would need to be redone every time the relative position of the scatterers changes.

In this paper, all validation work was done using spherical scatterers. This was done for comparison with analytical results that are readily available only for spherical scatterers. This model, however, is not limited to spherical scatterers only. Consequently, further numerical simulations will be performed for arbitrarily-shaped scatterers and the results will be reported in subsequent publications.

## II. PROBLEM FORMULATION

The simplest multiple-scattering problem is a two-scatterer problem as shown in Fig. 1. The same formulation procedure can be extended to cases where more than two scatterers are present. Two homogeneous scatterers, 1 and 2, characterized by the constitutive parameters  $(\mu_1, \epsilon_1)$  and  $(\mu_2, \epsilon_2)$ , respectively, can be of any arbitrary shape, orientation, and location. The external region  $e$  is characterized by the constitutive parameters  $(\mu_e, \epsilon_e)$ . The Stratton-Chu representation integrals [2] form the basis for deriving the governing BIE's for this problem. To derive the governing BIE's, the observation point  $P$  in the limit, is moved to each of the three surfaces,  $S_R$ ,  $S_1$ , and  $S_2$ .

As in the case of the single body scattering, any integration over the surface  $S_R$  goes to zero as  $R$  approaches infinity due to the radiation condition. Consequently, only two surfaces,  $S_1$  and  $S_2$ , need to be considered. Enforcing the boundary conditions at the scatterer surfaces

$$\hat{n}_1 \times \vec{E} = \hat{n}_1 \times \vec{E}_1 = -\vec{M}_1 \quad (1)$$

$$\hat{n}_1 \times \vec{H} = \hat{n}_1 \times \vec{H}_1 = \vec{J}_1 \quad (2)$$

$$\hat{n}_2 \times \vec{E} = \hat{n}_2 \times \vec{E}_2 = -\vec{M}_2 \quad (3)$$

$$\hat{n}_2 \times \vec{H} = \hat{n}_2 \times \vec{H}_2 = \vec{J}_2 \quad (4)$$

where  $\vec{J}$  and  $\vec{M}$  represent the equivalent surface electric and magnetic currents, respectively. The subscript indicates the surface under consideration.

The governing BIE's are [2]

$$\begin{aligned} & \frac{1}{2} \vec{M}_k(p) - \hat{n}_k(p) \times \nabla_p \times \int_{S_k} \vec{M}_k(q) G_e(p, q) dS_q \\ & + \frac{j}{\omega \epsilon_e} \hat{n}_k(p) \times \nabla_p \times \nabla_p \times \int_{S_k} \vec{J}_k(q) G_e(p, q) dS_q \\ & - \hat{n}_k(p) \times \nabla_p \times \int_{S_m} \vec{M}_m(q) G_e(p, q) dS_q \\ & + \frac{j}{\omega \epsilon_e} \hat{n}_k(p) \times \nabla_p \times \nabla_p \times \int_{S_m} \vec{J}_m(q) G_e(p, q) dS_q \\ & = -\hat{n}_k(p) \times \vec{E}_{\text{inc}}(p) = \vec{M}_{\text{inc}}(p) \end{aligned} \quad (5)$$

$$\begin{aligned} & \frac{1}{2} \vec{J}_k(p) - \hat{n}_k(p) \times \nabla_p \times \int_{S_k} \vec{J}_k(q) G_e(p, q) dS_q \\ & - \frac{j}{\omega \mu_e} \hat{n}_k(p) \times \nabla_p \times \nabla_p \times \int_{S_k} \vec{M}_k(q) G_e(p, q) dS_q \\ & - \hat{n}_k(p) \times \nabla_p \times \int_{S_m} \vec{J}_m(q) G_e(p, q) dS_q \\ & - \frac{j}{\omega \mu_e} \hat{n}_k(p) \times \nabla_p \times \nabla_p \times \int_{S_m} \vec{M}_m(q) G_e(p, q) dS_q \\ & = \hat{n}_k(p) \times \vec{H}_{\text{inc}}(p) = \vec{J}_{\text{inc}}(p) \end{aligned} \quad (6)$$

$$\begin{aligned} & \frac{1}{2} \vec{M}_k(p) + \hat{n}_k(p) \times \nabla_p \times \int_{S_k} \vec{M}_k(q) G_k(p, q) dS_q \\ & - \frac{j}{\omega \epsilon_k} \hat{n}_k(p) \times \nabla_p \times \nabla_p \times \int_{S_k} \vec{J}_k(q) G_k(p, q) dS_q \\ & = 0 \end{aligned} \quad (7)$$

$$\begin{aligned} & \frac{1}{2} \vec{J}_k(p) + \hat{n}_k(p) \times \nabla_p \times \int_{S_k} \vec{J}_k(q) G_k(p, q) dS_q \\ & + \frac{j}{\omega \mu_k} \hat{n}_k(p) \times \nabla_p \times \nabla_p \times \int_{S_k} \vec{M}_k(q) G_k(p, q) dS_q \\ & = 0 \end{aligned} \quad (8)$$

where  $k$  and  $m$  are equal to 1 and 2, but  $k \neq m$ .

The integration takes place over both surfaces and all subscripts are associated with the material of that region.  $\hat{n}$  is the outward pointing unit normal,  $G_\alpha$  is the free space Green's function

$$G_\alpha(p, q) = \frac{e^{jk_\alpha |p - q|}}{4\pi |p - q|} \quad (9)$$

$\omega$  is the frequency of the incident field, and  $\vec{M}_{\text{inc}}$  and  $\vec{J}_{\text{inc}}$  represent the cross product between the unit surface normal and the incident electric and magnetic fields, respectively. The scattered fields in the external region can be easily calculated by substituting the solutions obtained from (5)–(8) into the Stratton–Chu representation integral. There are more equations than there are unknowns, however, and to avoid the spurious resonance (eigenfrequency) problem [11], the Müller formulation is adopted. The resulting linear combinations are

$$\epsilon_e(5) - \epsilon_k(7) \quad (10)$$

$$\mu_e(6) - \mu_m(8). \quad (11)$$

This results in a set of four BIE's which is uniquely solvable at all frequencies.

### III. BIE REGULARIZATION

The particular regularization approach taken in this paper is the isolation technique [1]. This isolation process can be done either locally or globally. In both regularization approaches, the density function is expanded in a Taylor series about the collocation point. In the case of near singularity, the expansion is performed at an image point on the integration surface. The first one or two terms (depending on the order of the singularity) in the expansion are subtracted from the density function and added back, and the added-back terms are analytically transformed, using Stokes theorem, to nonsingular integrals. The assumption taken here is that the density function is at least Hölder continuous, and thus the difference between the two functions is of  $O(R)$  (or  $O(R^2)$  for the two term subtraction). The subtraction and addition of the expanded term(s) is done prior to taking the limit as the observation point approaches the collocation point on the surface. All integrals are at most weakly singular after the limit is taken. Consequently, there is no jump in the density function in the limit. The difference between the two approaches, however, is that for the global scheme, the added and subtracted terms involve integration over the entire surface, whereas in the local scheme, the added and subtracted terms involve integration over singular elements only. A singular element in this case is defined to be the element containing both the field point as well as the source point [19]. For the near-singular case, regularization of the high-order kernel functions to weakly singular kernel functions will result in well-behaved numerical solutions.

It should be emphasized that in both approaches, to properly regularize the hypersingular integrals, typically, a two-term addition and subtraction is needed. Examples of regularizing hypersingular kernels are found in [20]. As mentioned earlier, however, with the Müller formulation, the present regularization procedure requires only a one-term subtraction. The regularized forms of (5) using both global and local regularization techniques, expressed in index form, are shown in the following.

#### A. Global Regularization

$$\begin{aligned} -M_{it}(p) &= n_{jt}(p) \int_{S_t} \frac{\partial G_e(p, q)}{\partial x_i(q)} [M_{jt}(q) - M_{jt}(p)] dS_q \\ &- n_{jt}(p) \int_{S_t} \frac{\partial G_e(p, q)}{\partial x_j(q)} [M_{it}(q) - M_{it}(p)] dS_q \\ &+ M_{it}(p) \int_{S_t} \left[ \frac{\partial \vec{G}(p, q)}{\partial n_t(q)} - \frac{\partial G_e(p, q)}{\partial x_j(q)} n_{jt}(p) \right] dS_q \\ &+ \epsilon_{ijk} \frac{j}{\omega \epsilon_e} n_{jt}(p) \int_{S_t} \frac{\partial^2 G_e(p, q)}{\partial x_m(q) \partial x_k(q)} j_{mt}(q) dS_q \\ &+ \epsilon_{ijk} j \omega \mu_e n_{jt}(p) \int_{S_t} G_e(p, q) J_{kt}(q) dS_q \\ &+ n_{jt}(p) \int_{S_c} \frac{\partial G_e(p, q)}{\partial x_i(q)} M_{jc}(q) dS_q \\ &- n_{jt}(p) \int_{S_c} \frac{\partial G_e(p, q)}{\partial x_j(q)} M_{ic}(q) dS_q \end{aligned}$$

$$\begin{aligned}
 & + \epsilon_{ijk} \frac{j}{\omega \epsilon_e} n_{jt}(p) \int_{S_c} \frac{\partial^2 G_e(p, q)}{\partial x_m(q) \partial x_k(q)} J_{mc}(q) dS_q \\
 & + \epsilon_{ijk} j \omega \mu_e n_{jt}(p) \int_{S_c} G_e(p, q) J_{kc}(q) dS_q \\
 & - M_{it}^{\text{inc}}(p).
 \end{aligned} \tag{12}$$

### B. Local Regularization

$$\begin{aligned}
 -\frac{1}{2} M_{it}(p) & = n_{jt}(p) \int_{S_i - \Delta S} \frac{\partial G_e(p, q)}{\partial x_i(q)} M_{jt}(q) dS_q \\
 & - n_{jt}(p) \int_{S_i - \Delta S} \frac{\partial G_e(p, q)}{\partial x_j(q)} M_{it}(q) dS_q \\
 & + \epsilon_{ijk} \frac{j}{\omega \epsilon_e} n_{jt}(p) \int_{S_i} \frac{\partial^2 G_e(p, q)}{\partial x_m(q) \partial x_k(q)} \\
 & \cdot J_{mt}(q) dS_q + \epsilon_{ijk} j \omega \mu_e n_{jt}(p) \\
 & \cdot \int_{S_i} G_e(p, q) J_{kt}(q) dS_q \\
 & + n_{jt}(p) \int_{\Delta S} \frac{\partial G_e(p, q)}{\partial x_i(q)} [M_{jt}(q) - M_{jt}(p)] dS_q \\
 & + \int_{\Delta S} \left[ \frac{\partial \bar{G}(p, q)}{\partial n_t(q)} M_{it}(p) \right. \\
 & \left. - \frac{\partial G_e(p, q)}{\partial x_j(q)} n_{jt}(p) M_{it}(q) \right] dS_q \\
 & - M_{it}(p) \int_{\Delta S} \frac{\partial \bar{G}(p, q)}{\partial n_t(q)} dS_q \\
 & + n_{jt}(p) \int_{S_c} \frac{\partial G_e(p, q)}{\partial x_i(q)} M_{jc}(q) dS_q \\
 & - n_{jt}(p) \int_{S_c} \frac{\partial G_e(p, q)}{\partial x_j(q)} M_{ic}(q) dS_q \\
 & + \epsilon_{ijk} \frac{j}{\omega \epsilon_e} n_{jt}(p) \int_{S_c} \frac{\partial^2 G_e(p, q)}{\partial x_m(q) \partial x_k(q)} \\
 & \cdot J_{mc}(q) dS_q + \epsilon_{ijk} j \omega \mu_e n_{jt}(p) \\
 & \cdot \int_{S_c} G_e(p, q) J_{kc}(q) dS_q - M_{it}^{\text{inc}}(p). \tag{13}
 \end{aligned}$$

Here  $\bar{G}$  is the static Greens function,  $\epsilon$  is the permutation symbol, and  $\Delta S$  is the singular element on which both  $p$  and  $q$  reside. All of the integrals above are at most weakly singular. This weak singularity is finally removed by mapping from Cartesian to a local polar coordinate system. The mapping process changes the integration parameters from  $(dx dy)$  to  $(\rho \sin \theta d\rho d\theta)$  where the  $\rho$  cancels out the weakly singular kernel of  $O(1/R)$ . The end result after the mapping is a regular integral which can be easily evaluated using Gaussian quadrature with unit weight factor. The regularized forms of (6)–(8) are similar to (12) and (13) and can be obtained using the same procedure.

## IV. NUMERICAL RESULTS

The new BIE's with regularized kernel functions can be used to solve both single scattering problems and multiple scattering problems. We tested this method for both types of problems with excellent results. In all of our numerical

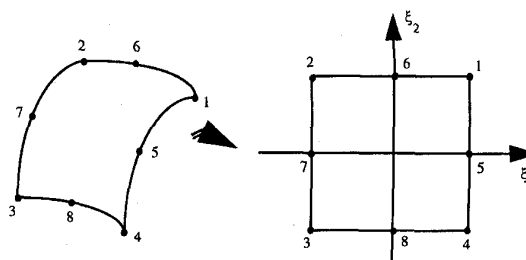


Fig. 2. Mapping from a curvilinear element to a local square element.

simulations, scalar quadratic basis functions were used to interpolate the geometry information and the unknown density functions. This differs from the vector basis functions approach used in [10] where the nodal unknowns are scalar quantities. In our approach, the nodal unknowns are the actual vector components of the current densities. In addition, curvilinear elements were used to mesh the scatterer surface. Specifically, two shapes of elements were used in the simulation. These are the quadrilateral elements which contain eight nodes per element and triangular elements which contain six nodes per element. The quadratic basis functions for quadrilateral elements are given in (14)–(21). These functions are used to map the curvilinear elements to a planar square surface defined from  $-1$  to  $1$  along each axis. The location of the nodes are shown in Fig. 2. The expansion of the geometry information and the density functions are given in (22)–(23), respectively

$$N^1(\vec{\xi}) = \frac{1}{4}(\xi_1 + 1)(\xi_2 + 1)(\xi_1 + \xi_2 - 1) \tag{14}$$

$$N^2(\vec{\xi}) = \frac{1}{4}(\xi_1 - 1)(\xi_2 + 1)(\xi_1 - \xi_2 + 1) \tag{15}$$

$$N^3(\vec{\xi}) = \frac{1}{4}(1 - \xi_1)(\xi_2 - 1)(\xi_1 + \xi_2 + 1) \tag{16}$$

$$N^4(\vec{\xi}) = \frac{1}{4}(\xi_1 + 1)(\xi_2 - 1)(-\xi_1 + \xi_2 + 1) \tag{17}$$

$$N^5(\vec{\xi}) = \frac{1}{2}(\xi_1 + 1)(1 - \xi_2^2) \tag{18}$$

$$N^6(\vec{\xi}) = \frac{1}{2}(\xi_2 + 1)(1 - \xi_1^2) \tag{19}$$

$$N^7(\vec{\xi}) = \frac{1}{2}(\xi_1 - 1)(\xi_2^2 - 1) \tag{20}$$

$$N^8(\vec{\xi}) = \frac{1}{2}(1 - \xi_2)(1 - \xi_1^2) \tag{21}$$

$$x_i(\xi_1, \xi_2) = \sum_{\alpha=1}^m N^\alpha(\xi_1, \xi_2) x_i^\alpha \tag{22}$$

$$M_i(\xi_1, \xi_2) = \sum_{\alpha=1}^m N^\alpha(\xi_1, \xi_2) M_i^\alpha \tag{23}$$

where  $(\xi_1, \xi_2)$  are the local coordinates defined on the planar square surface,  $m$  is the number of nodes on an element,  $i$  represents the component in Cartesian system, and  $M_i^\alpha(x_i^\alpha)$  represents the quantity defined on the node  $\alpha$ . As can be seen from (14)–(21), all three components of the surface current density are continuous across adjacent elements. The same observation is also made for basis functions defined on the curvilinear triangular elements [19].

We first tested the new approach on single scattering problems. It is our experience that typically, it takes about three to four elements per free-space wavelength in each dimension

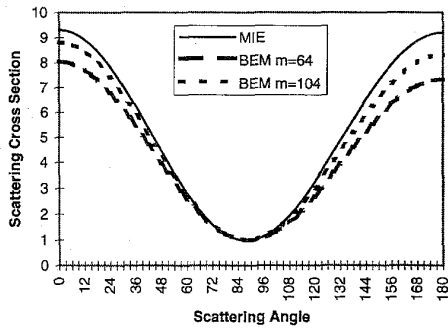


Fig. 3. Scattering cross section versus  $\theta$  for a single sphere. Index of refraction  $N = 4.0$ ,  $ka = 1.0$ .

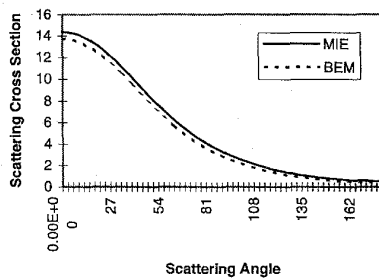


Fig. 4. Scattering cross section versus  $\theta$  for a single sphere. Index of refraction  $N = 2.0$ ,  $ka = 1.5$ .

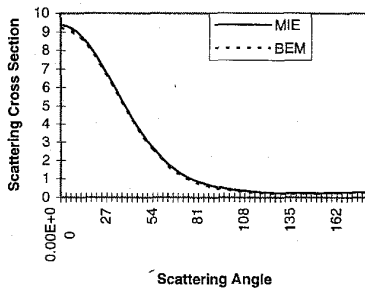


Fig. 5. Scattering cross section versus  $\theta$  for a single sphere. Index of refraction  $N = 1.5$ ,  $ka = 2.0$ .

to adequately discretize the scatterer surface with refractive index of two or less. Naturally, this number will increase as the refractive index of the scatterer increases. Currently, we determine the required mesh density experimentally for materials with  $N > 2$ . The exact relation between the mesh density and the scatterer's refractive index is still under study. In this test, the scatterer is consistently discretized into 64 surface elements ( $m = 64$ ) with 178 nodes ( $n = 178$ ) for convenience. Figs. 3–6 illustrate the scattering cross section versus the scattering angle plotted against analytical solutions obtained using the Mie theory [17]. As can be seen from the plots, there is an excellent agreement between our solutions and the analytical solutions for a wide range of permittivities. The maximum percentage error for the case of  $\epsilon_r = 16$  ( $N = 4$ ) is about 13 percent for  $m = 64$ . As we increased the number of elements from  $m = 64$  to  $m = 104$  ( $n = 288$ ), the error reduced to about 5 percent. Indeed, the error can be lowered

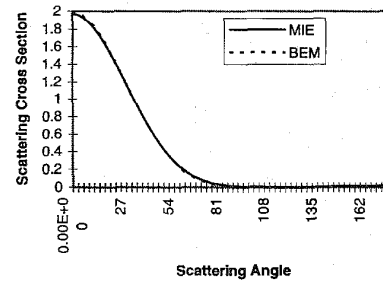


Fig. 6. Scattering cross section versus  $\theta$  for a single sphere. Index of refraction  $N = 1.2$ ,  $ka = 2.2$ .

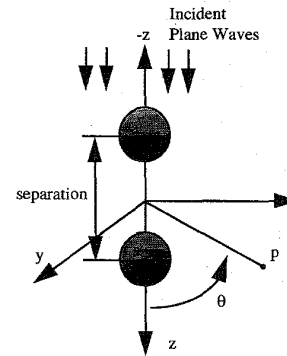


Fig. 7. Test configuration for the two-scatterer problem. The vertical intensity is calculated in the  $x$ - $z$  plane as a function of  $\theta$ , where  $\theta$  is measured from the  $z$ -axis. The incident field is a unit-amplitude plane wave polarized in the  $+y$  direction, traveling in the  $+z$  direction.

with a finer meshed surface. The percentage errors for the other test cases are lower. Next, we tested our approach on multiple scattering problems. To compare the BIE solutions with published results, two identical spherical scatterers are used. The test configuration for the two-scatterer problem is shown in Fig. 7. This is the test configuration used in [21] to illustrate the analytical scattering solutions for two spheres. The incident fields are unit-amplitude plane waves polarized in the  $y$ -direction. The refractive index for both scatterers is taken to be 1.2 and the radii and the separation between the spheres are expressed in terms of the dimensionless quantity  $ka$ , where  $a$  is the radius of the spheres. The scattered waves are calculated in the far-field region in the  $x$ - $z$  plane as a function of  $\theta$ . In this test, each sphere is discretized into 16 elements consisting of both quadrilateral and triangular elements for a total of 112 nodes on each sphere. The tests were done on a DEC 5000/240 workstation with about 10–15 minutes per configuration run. The results are shown in Figs. 8 and 9 for various separations and radii of the spheres. The BIE solutions are plotted against the solutions at discrete locations obtained by [21] using the modal expansion method. The vertical intensity is calculated by dividing the scattered fields obtained from the two scatterer problem by the scattered fields obtained from the single scatterer problem. In the plots, the vertical axis represents the vertical intensity and the horizontal axis represents the scattering angle  $\theta$ . The two solutions are in excellent agreement which clearly demonstrates the accuracy of the BIE method.

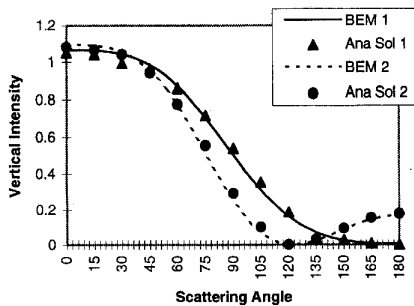


Fig. 8. Vertical intensity versus  $\theta$  for spheres having a radius of  $ka = 0.5$ . The refractive index of the spheres is  $N = 1.2$ . #1 separation =  $3a$ . #2 separation =  $4a$ .

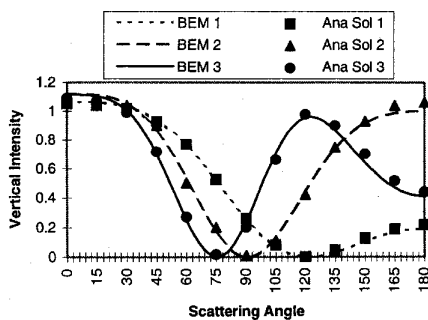


Fig. 9. Vertical intensity versus  $\theta$  for spheres having a radius of  $ka = 1.0$ . The refractive index of the spheres is  $N = 1.2$ . #1 separation =  $2a$ . #2 separation =  $3a$ . #3 separation =  $4a$ .

V. CONCLUSIONS

A regularized BIE approach for electromagnetic scattering problems is presented. The approach is versatile in dealing with any BIE formulations for calculating the scattered fields due to arbitrarily-shaped scatterers with arbitrary orientation. Major difficulties in handling singular integrals commonly associated with integral-equation methods has been overcome by reducing the order of singularity in the kernel function using an effective regularization process. This approach is valid for any order of singularity. It also works for a near-singularity. There are two major advantages of regularizing singular integrals. First, the process eliminates the need to calculate the surface divergence of density functions or the need of introducing additional unknowns. Second, no analytical interpretation or evaluation of CPV's is needed. Thus, curvilinear elements can be used too, and there is no need to approximate curved surfaces with flat elements. Accurate numerical solutions have been obtained which are in excellent agreement with analytical solutions. The test of the BIE method for irregularly-shaped scatterers will be performed and compared with experimental measurements. The results will be reported later.

REFERENCES

[1] G. Krishnasamy, F. J. Rizzo, and T. J. Rudolph, "Hypersingular integral equations: Their occurrence, interpretation, regularization and computation," in *Developments in BEM*, vol. 7, Feb. 1991.

[2] P. A. Martin and P. Ola, "Boundary integral equations for the scattering of electromagnetic waves by homogeneous dielectric obstacles," in *Proc. Royal Society Edinburgh*, vol. 123A, pp. 185-208, 1993.

[3] W. S. Hall, X. Mao, and W. Robertson, "Quadratic, isoparametric BEM formulation for electromagnetic scattering from arbitrarily shaped three-dimensional homogeneous dielectric objects," in *Boundary Elements XIV*, C. A. Brebbia, J. Dominguez, and F. Parvis, Eds. Southampton: Computational Mechanics Pub., 1992.

[4] M. S. Ingber and R. H. Ott, "An application of the boundary element method to the magnetic field integral equation," *IEEE Trans. Antennas Propagat.*, vol. 39, pp. 606-611, May 1991.

[5] J. R. Mautz, "A stable integral equation for electromagnetic scattering from homogeneous dielectric bodies," *IEEE Trans. Antennas Propagat.*, vol. 37, pp. 1070-1071, Aug. 1987.

[6] E. Marx, "Integral equation for scattering by a dielectric," *IEEE Trans. Antennas Propagat.*, vol. AP-32, pp. 166-172, Feb. 1984.

[7] A. Glisson, "An integral equation for electromagnetic scattering from homogeneous dielectric bodies," *IEEE Trans. Antennas Propagat.*, vol. AP-32, pp. 173-175, Feb. 1984.

[8] R. F. Harrington, "Boundary integral formulations for homogeneous material bodies," *J. Electromagnetic Waves Appl.*, vol. 3, pp. 1-5, 1989.

[9] J. M. Putnam, "Combined-field formulation for conducting bodies with thin coatings," *Appl. Computational Electromagnetics Soc. J.*, Fall 1989, pp. 15-26.

[10] K. Umashankar, A. Taflov, and S. M. Rao, "Electromagnetic scattering by arbitrary shaped three-dimensional lossy dielectric objects," *IEEE Trans. Antennas Propagat.*, vol. AP-34, pp. 758-765, June 1986.

[11] J. R. Mautz and R. F. Harrington, "Electromagnetic scattering from a homogeneous body of revolution," *Achiv Für Elektronik und Übertragungstechnik*, vol. 33, pp. 71-80, 1979.

[12] N. Morita, "Surface integral representations for electromagnetic scattering from dielectric cylinders," *IEEE Trans. Antennas Propagat.*, vol. AP-26, pp. 261-266, Mar. 1978.

[13] T. K. Wu and L. L. Tsai, "Electromagnetic fields inside arbitrary cylinders of biological tissue," *IEEE Trans. Microwave Theory Tech.*, Jan. 1977, pp. 61-65.

[14] E. Marx, "Electromagnetic scattering from a dielectric wedge and the single hypersingular integral equation," *IEEE Trans. Antennas Propagat.*, vol. 41, pp. 1001-1008, Aug. 1993.

[15] E. J. Bawolek and E. D. Hirtleman, "Light scattering by submicron spherical particles on semiconductor surfaces," in *Particles on Surfaces*, K. Mittal, Ed. New York: Plenum, 1991.

[16] P. Spyak and W. L. Wolfe, "Scatter from particulate contaminated mirrors," *Optical Eng.*, vol. 31, pp. 1746-1763, Aug. 1992.

[17] C. F. Bohren and D. R. Huffman, *Absorption and Scattering of Light by Small Particles*. New York: Wiley, 1983.

[18] H. C. Van de Hulst, *Light Scattering by Small Particles*. New York: Dover, 1957.

[19] J. C. Chao, "A boundary integral equation approach to three-dimensional electromagnetic wave scattering problems," Ph.D. dissertation, Iowa State Univ., May 1994.

[20] J. C. Chao, Y. J. Liu, F. J. Rizzo, and N. Nakagawa, "A boundary integral equation approach for solving eddy currents around a fully-embedded crack inside a conducting tubing wall," in *1995 Progress in Electromagnetics Research Symp.*, July 1995.

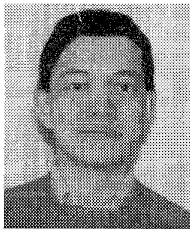
[21] S. Levine and G. O. Olaofe, "Scattering of electromagnetic waves by two equal spherical particles," *J. Colloid and Interface Sci.*, vol. 27, pp. 442-457, July 1968.



**Joseph C. Chao** (S'85) received the B.S. degree in electrical engineering from Colorado State University, Fort Collins, in 1988, and the M.S. and Ph.D. degrees in electrical engineering from Iowa State University, Ames, in 1991 and 1994, respectively.

From 1988-1990, he worked as a Reliability Engineer at the Avionics Systems of Texas Instruments, Inc., in Plano, Texas. He is currently working as a Postdoctoral Fellow at the Center for Nondestructive Evaluation, Ames, Iowa. His research interests include the area of numerical

modeling of electromagnetic NDE techniques. Dr. Chao is a member of Phi Kappa Phi, Tau Beta Pi, and Eta Kappa Nu. He is also an associate member of Sigma Xi.

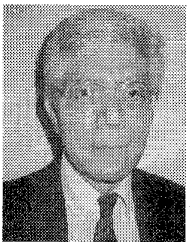


**Yijun J. Liu** received the B.S. degree in 1981 and the M.S. degree in 1984, both in aerospace engineering, from Northwestern Polytechnical University in Xian, China. He obtained the Ph.D. degree in 1992 in theoretical and applied mechanics from the University of Illinois at Urbana-Champaign.

He is currently working in the automobile industry with the Automated Analysis Corporation in Ann Arbor, MI. His research interest has been in computational mechanics, especially the boundary integral equation/boundary element method (BIE/BEM). He

has published several papers in journals on the boundary element method for plate bending, nonlinear deformation, elastic buckling, acoustic, elastodynamic, and electromagnetic problems.

Dr. Liu is a member of IACM, USACM, and IABEM and an associate member of ASME and SAE.

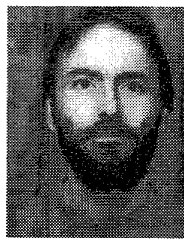


**Frank J. Rizzo** received the B.S. degree in civil engineering and the M.S. and Ph.D. degrees in theoretical and applied mechanics at the University of Illinois, Urbana.

He has held faculty positions at the University of Washington, Seattle, and the University of Kentucky, Lexington, and has been a Professor and chairman of the Mechanics Department at the University of Illinois, and Iowa State University. He is a member of several editorial boards of journals for computational methods in mechanics

and engineering. His research interests include computational methods for engineering problems with particular emphasis on boundary element methods for acoustic, ultrasonic, and electromagnetic wave scattering. His longtime involvement with boundary element methods has given him opportunities to give seminars and workshops in universities, industries, and government laboratories in the United States, Europe, and Asia.

Dr. Rizzo was awarded the Warner Medal for an outstanding contribution to the permanent literature of engineering by the American Society of Mechanical Engineers in 1993. He is a member of the American Society of Mechanical Engineers, the American Academy of Mechanics, the Society for Industrial and Applied Mathematics, the International and United States Associations for Computational Mechanics, the International Association for Boundary Element Methods, and a member of several honor societies: Chi Epsilon, Tau Beta Pi, Sigma Tau, and Sigma Xi.



**Paul A. Martin** was born in London, England, in 1954. He received the B.Sc. degree in mathematics from the University of Bristol in 1975, and the M.Sc. and Ph.D. degrees from the University of Manchester in 1976 and 1980, respectively.

His research interests include scattering theory, fracture mechanics, and integral equations. He is currently a Reader in the Department of Mathematics at the University of Manchester.



**Lalita Udpa** (S'84-M'86-SM'91) received the M.S. and Ph.D. degrees from the department of electrical engineering at Colorado State University, Fort Collins, in 1981 and 1986, respectively.

She is currently an Associate Professor at the Department of Electrical and Computer Engineering at Iowa State University. Her teaching and research interests include numerical modeling and analysis, application of signal processing to nondestructive evaluation problems, and neural networks.